2011

Excitation of Rydberg States in Rubidium with Near Infrared Diode Lasers

Donald Fahey
Bryn Mawr College, dfahey@brynmawr.edu

Michael Noel
Bryn Mawr College, mnoel@brynmawr.edu

Custom Citation
D.P. Fahey and M.W. Noel, *Optics Express* **19**, 17002 (2011).

Excitation of Rydberg states in rubidium with near infrared diode lasers

Donald P. Fahey and Michael W. Noel

Department of Physics, Bryn Mawr College, Bryn Mawr, Pennsylvania 19010, USA

*mnoel@brynmawr.edu

Abstract: A system of three external cavity diode lasers is used to excite Rydberg states in rubidium. The 5S→5P→5D transitions are driven using lasers with $\lambda = 780$ and 776 nm respectively. From the 5D state, atoms fluoresce down to the 6P state. The final transition to Rydberg levels is from the 6P state with laser light near $\lambda = 1016$ nm. The *n*S and *n*D Rydberg states are accessible directly and with the application of a modest electric field *n*P states can also be excited. As a test of this system, Stark spectra are collected for *n*D and *n*P states.

OCIS codes: (020.5780) Rydberg states; (140.2020) Diode lasers.

References and links

1. W. R. Anderson, J. R. Veale, and T. F. Gallagher, "Resonant dipole–dipole energy transfer in a nearly frozen Rydberg gas," Phys. Rev. Lett. **80**, 249–252 (1998).
2. I. Mourachko, D. Comparat, F. de Tomasi, A. Fioretti, P. Nosbaum, V. M. Akulin, and P. Pillet, "Many-body effects in a frozen Rydberg gas," Phys. Rev. Lett. **80**, 253-256 (1998).
3. D. Tong, S. M. Farooqi, J. Stanojevic, S. Drishnan, Y. P. Zhang, R. Côté, E. E. Eyler, and P. L. Gould, "Local blockade of Rydberg excitation in an ultracold gas," Phys. Rev. Lett. **93**, 063001 (2004).
4. T. Vogt, M. Viteau, J. Zhao, A. Chotia, D. Comparat, and P. Pillet, "Dipole blockade at Förster resonances in high-resolution laser excitation of Rydberg states of cesium atoms," Phys. Rev. Lett. **97**, 083003 (2006).
5. E. Urban, T. A. Johnson, T. Henage, L. Isenhower, D. D. Yavuz, T. G. Walker, and M. Saffman, "Observation of Rydberg blockade between two atoms," Nat. Phys. **5**, 110–114 (2009).
6. A. Gaëtan, Y. Miroshnychenko, T. Wilk, A. Chotia, M. Viteau, D. Comparat, P. Pillet, A. Browaeys, and P. Grangier,"Observation of collective excitation of two individual atoms in the Rydberg blockade regime," Nat. Phys. **5**, 115–118 (2009).
7. D. Comparat and P. Pillet, "Dipole blockade in a cold Rydberg atomic sample [Invited]," J. Opt. Soc. Am. B **27**, A208–A232 (2010).
8. M. D. Lukin and P. R. Hemmer, "Quantum entanglement via optical control of atom–atom interactions," Phys. Rev. Lett. **84**, 2818-2821 (2000).
9. D. Jaksch, J. I. Cirac, P. Zoller, S. L. Rolston, R. Côté, and M. D. Lukin, "Fast quantum gates for neutral atoms," Phys. Rev. Lett. **85**, 2208–2211 (2000).
10. M. Saffman, T. G. Walker, and K. Mølmer, "Quantum information with Rydberg atoms," Rev. Mod. Phys. **82**, 2313-2363 (2010).
11. L. Isenhower, E. Urban, X. L. Zhang, A. T. Gill, T. Henage, T. A. Johnson, T. G. Walker, and M. Saffman, "Demonstration of a neutral atom controlled-NOT quantum gate," Phys. Rev. Lett. **104**, 010503 (2010).
12. T. Wilk, A. Gaëtan, C. Evellin, J. Wolters, Y. Miroshnychenko, P. Grangier, and A. Browaeys, "Entanglement of two individual neutral atoms using Rydberg blockade," Phys. Rev. Lett. **104**, 010502 (2010).
13. A. Fioretti, D. Comparat, C. Drag, T. F. Gallagher, and P. Pillet, "Long-range forces between cold atoms," Phys. Rev. Lett. **82**, 1839–1842 (1999).
14. M. P. Robinson, B. Laburthe Tolra, Michael W. Noel, T. F. Gallagher, and P. Pillet, "Spontaneous evolution of Rydberg atoms into an ultracold plasma," Phys. Rev. Lett. **85**, 4466–4469 (2000).
15. S. K. Dutta, D. Feldbaum, A. Walz-Flannigan, J. R. Guest, and G. Raithel, "High-angular-momentum states in cold Rydberg gasses," Phys. Rev. Lett. **86**, 3993–3996 (2001).
16. T. C. Killian, T. Pattard, T. Pohl and J. M. Rost, "Ultracold neutral plasmas," Phys. Rep. **449**, 77–130 (2007).

#147515 - $15.00 USD Received 13 May 2011; revised 27 Jun 2011; accepted 31 Jul 2011; published 16 Aug 2011

17. C. Boisseau, I. Simbotin, and R. Côté, "Macrodimers: ultralong range Rydberg molecules," Phys. Rev. Lett. **88**, 133004 (2002).
18. S. M. Farooqi, D. Tong, S. Krishnan, J. Stanojevic, Y. P. Zhang, J. R. Ensher, A. S. Estrin, C. Boisseau, R. Côté, E. E. Eyler, and P. L. Gould, "Long-range molecular resonances in a cold Rydberg gas," Phys. Rev. Lett. **91**, 183002 (2003).
19. K. R. Overstreet, A. Schwettmann, J. Tallant, D. Booth, and J. P. Shaffer, "Observation of electric-field-induced Cs Rydberg atom macrodimers," Nat. Phys. **5**, 581–585 (2009).
20. C. H. Greene, A. S. Dickinson, and H. R. Sadeghpour, "Creation of polar and nonpolar ultra-long-range Rydberg molecules," Phys. Rev. Lett. **85**, 2458–2461 (2000).
21. V. Bendowsky, B. Butscher, J. Nipper, J. P. Shaffer, R. Löw, and T. Pfau, "Observation of ultralong-range Rydberg molecules," Nature **458**, 1005–1008 (2009).
22. V. Bendkowsky, B. Butscher, J. Nipper, J. B. Balewski, J. P. Shaffer, R. Löw, T. Pfau, W. Li, J. Stanojevic, T. Pohl, and J. M. Rost, "Rydberg trimers and excited dimers bound by internal quantum reflection," Phys. Rev. Lett. **105**, 163201 (2010).
23. K. B. MacAdam, A. Steinbach, and C. Wieman, "A narrow-band tunable diode laser system with grating feedback and a saturated absorption spectrometer for Cs and Rb," Am. J. Phys. **60**, 1098–1111 (1992).
24. C. Iu, G. D. Stevens, and H. Metcalf, "Instrumentation for multistep excitation of lithium atoms to Rydberg states," Appl. Opt. **34**, 2640–2644 (1995).
25. A. Grabowski, R. Heidemann, R. Löw, J. Stuhler, and T. Pfau, "High resolution Rydberg spectroscopy of ultracold rubidium atoms," Fortschr. Phys. **54**, 765–775 (2006).
26. M. Viteau, J. Radogostowicz, M. G. Bason, N. Malossi, D. Ciampini, O. Morsch, and E. Arimondo, "Rydberg spectroscopy of a Rb MOT in the presence of applied or ion created electric fields," Opt. Express **19**, 6007–6019 (2011).
27. P. Thoumany, Th. Germann, T. Hänsch, G. Stania, L. Urbonas, and Th. Becker, "Spectroscopy of rubidium Rydberg states with three diode lasers," J. Mod. Opt. **56**, 2055–2060 (2009).
28. B. Sanguinetti, H. O. Majeed, M. L. Jones, and B. T. H. Varcoe, "Precision measurements of quantum defects in the $n\mathrm{P}_{3/2}$ Rydberg states of ^{85}Rb," J. Phys. B **42**, 165004 (2009).
29. L. A. M. Johnson, O. H. Majeed, B. Sanguinetti, Th. Becker, and B. T. H. Varcoe, "Absolute frequency measurements of ^{85}Rb $n\mathrm{F}_{7/2}$ Rydberg states using purely optical detection," New J. Phys. **12**, 063028 (2010).
30. T. T. Grove, V. Sanchez-Villicana, B. C. Duncan, S. Maleki, and P. L. Gould, "Two-photon two-color diode laser spectroscopy of the Rb $5D_{5/2}$ state," Phys. Scr. **52**, 271–276 (1995).
31. T. Meijer, J. D. White, B. Smeets, M. Jeppesen, and R. E. Scholten, "Blue five-level frequency-upconversion system in rubidium," Opt. Lett. **31**, 1002–1004 (2006).
32. W. Süptitz, B. C. Duncan, and P. L. Gould, "Efficient 5*D* excitation of trapped Rb atoms using pulses of diode-laser light in the counterintuitive order," J. Opt. Soc. Am. B **14**, 1001–1008 (1997).
33. E. Paradis, B. Barrett, A. Kumarakrishnan, R. Zhang, and G. Raithel, "Observation of superfluorescent emissions from laser-cooled atoms," Phys. Rev. A **77**, 043419 (2008).
34. D. Sheng, A. Pérez Galván, and L. A. Orozco, "Lifetime measurements of the 5*d* states of rubidium," Phys. Rev. A **78**, 062506 (2008).
35. E. Gomez, S. Aubin, L. A. Orozco, and G. D. Sprouse, "Lifetime and hyperfine splitting measurements on the 7*s* and 6*p* levels in rubidium," J. Opt. Soc. Am. B **21**, 2058–2067 (2004).
36. A. J. Olson and S. K. Mayer, "Electromagnetically induced transparency in rubidium," Am. J. Phys. **77**, 116–121 (2009).
37. A. Hemmerich, D. H. McIntyre, C. Zimmermann, T. W. Hänsch, "Second-harmonic generation and optical stabilization of a diode laser in an external ring resonator," Opt. Lett. **15**, 372–374 (1990).
38. M. L. Zimmerman, M. G. Littman, M. M. Kash, and D. Kleppner, "Stark structure of the Rydberg states of alkali-metal atoms," Phys. Rev. A **20**, 2251–2275 (1979).
39. W. Li, I. Mourachko, M. W. Noel, and T. F. Gallagher, "Millimeter-wave spectroscopy of cold Rb Rydberg atoms in a magneto-optical trap: quantum defects of the *ns*, *np*, and *nd* series," Phys. Rev. A **67**, 052502 (2003).
40. M. S. Safronova, C. J. Williams, and C. W. Clark,"Relativistic many-body calculations of electric-dipole matrix elements, lifetimes, and polarizabilities in rubidium," Phys. Rev. A **69**, 022509 (2004).
41. S. K. Dutta, D. Feldbaum, A. Walz-Flannigan, J. R. Guest, and G. Raithel, "High-angular-momentum states in cold Rydberg gasses," Phys. Rev. Lett. **86**, 3993–3996 (2001).
42. W. Li, M. W. Noel, M. P. Robinson, P. J. Tanner, T. F. Gallagher, D. Comparat, B. Laburthe Tolra, N. Vanhaecke, T. Vogt, N. Zahzam, P. Pillet, and D. A. Tate, "Evolution dynamics of a dense frozen Rydberg gas to plasma," Phys. Rev. A **70**, 042713 (2004).

Diode lasers are a useful tool for high-resolution spectroscopy due to their narrowband output, tunability, low-cost, and ease-of-use. Since their introduction to atomic spectroscopy they have become a promising alternative to high-power, pulsed lasers for the purpose of exciting high-lying Rydberg states in alkali metal atoms. The exaggerated properties of Rydberg atoms

#147515 - $15.00 USD Received 13 May 2011; revised 27 Jun 2011; accepted 31 Jul 2011; published 16 Aug 2011

have been exploited in a number of recent experiments with ultracold atoms. Their large polarizabilities allow pairs of Rydberg atoms to interact strongly over distances of several microns. With the application of a small electric field, a dipole-dipole energy exchange between pairs of atoms can be tuned into resonance [1, 2]. This interaction can also lead to a blockade effect, which limits the number of excited Rydberg atoms [3, 4] and can even limit the excitation in a small sample to a single Rydberg atom [5–7]. Ultimately the Rydberg blockade may be useful in building a quantum computer [8–12]. In addition to allowing Rydberg atoms to exchange energy, the dipole-dipole interaction also results in a mechanical force between pairs of atoms. This force can cause atoms to collide, ionizing the weakly bound electrons, and leading to the formation of an ultracold plasma [13–16]. The extremely low collision energies between ultracold atoms also makes possible the formation of exotic ultralong-range Rydberg molecules. In one example of these exotic molecules, a pair of Rydberg atoms is bound together forming a macrodimer with a size greater than 1 μm [17–19]. In a second example, a ground state atom is trapped in a shallow potential well formed by the Rydberg electron of a second atom [20–22].

In this work, we demonstrate a diode laser system for use in populating Rydberg states of rubidium atoms in a magneto-optical trap (MOT). As a test of our laser system, we report spectroscopy of low-angular momentum, high principal quantum number Rydberg states, and observe the Stark splitting in the presence of a dc electric field. Grating feedback can reduce the output bandwidth of external cavity diode lasers (ECDLs) to the kilohertz range, and conventional locking techniques can ensure frequency stabilization to sub-megahertz levels [23]. Advances in mount design and assembly have made it possible to tune ECDLs single-mode over tens of nanometers, making them suitable for high-resolution spectroscopy. The lack of widely tunable ultraviolet wavelength diode lasers required for the direct excitation from the ground state to Rydberg states has led to the use of multistep processes involving visible and near-infrared wavelengths. An early example of this is an experiment by Iu, *et al.* [24]. Lithium atoms in an atomic beam were excited to $n \simeq 15$ states by a three-step 2S$\rightarrow$2P$\rightarrow$3S$\rightarrow n$P ladder-type process. Diode lasers operating at $\lambda = 671$ nm and $\lambda = 813$ nm were locked to the 2S$\rightarrow$2P and 2P$\rightarrow$3S transitions, respectively, while a third diode laser was tuned to the $n = 15$ manifold. Through a combination of photoionization and field ionization they were able to detect Stark resonances in an electric field, thereby showing that low-power near-infrared cw diode lasers can be used for Rydberg excitation.

In the case of rubidium, several multi-step diode laser systems have been developed possessing a range of advantages and disadvantages. Due to dipole selection rules and the energy level spacings of rubidium (both ^{85}Rb and ^{87}Rb), pathways using visible single photon transitions for the first step are limited to the transitions 5S$\rightarrow$5P at $\lambda = 780$ nm or 5S$\rightarrow$6P at $\lambda = 421$ nm. The first of these is often used because of the commercial availability of lasers operating near $\lambda = 780$ nm. For two-step excitation, this means that the final step to Rydberg levels requires wavelengths near $\lambda = 480$ nm. While laser diodes operating at blue wavelengths are available, in practice it can be advantageous to frequency-double a longer wavelength laser. One example where this was realized is Grabowski, *et al.* [25], who used this excitation scheme to probe the Stark splitting of the ^{87}Rb 41D doublet in a MOT. In this case, an injection-locked frequency-doubled $\lambda = 960$ nm diode laser was used to generate the $\lambda = 480$ nm light needed for the second step. Alternatively, the 5S$\rightarrow$6P$\rightarrow n$S,nD pathway requires blue laser light for the first transition and light near $\lambda = 1015$ nm for the second [26]. In this case the $\lambda = 421$ nm light is generated by doubling the amplified light from a 842 nm diode laser.

The need for blue wavelengths is avoided altogether with a three-step diode laser system. For instance, Thoumany, *et al.*, used the 5S$\rightarrow$5P$\rightarrow$5D$\rightarrow n$P pathway to excite Rydberg states in ^{85}Rb [27]. All three transitions use light in the near-IR, with $\lambda = 780$ nm, 776 nm, and $\sim$1260 nm. This pathway was also used by Sanguinetti *et al.* to measure the quantum defects

#147515 - $15.00 USD Received 13 May 2011; revised 27 Jun 2011; accepted 31 Jul 2011; published 16 Aug 2011

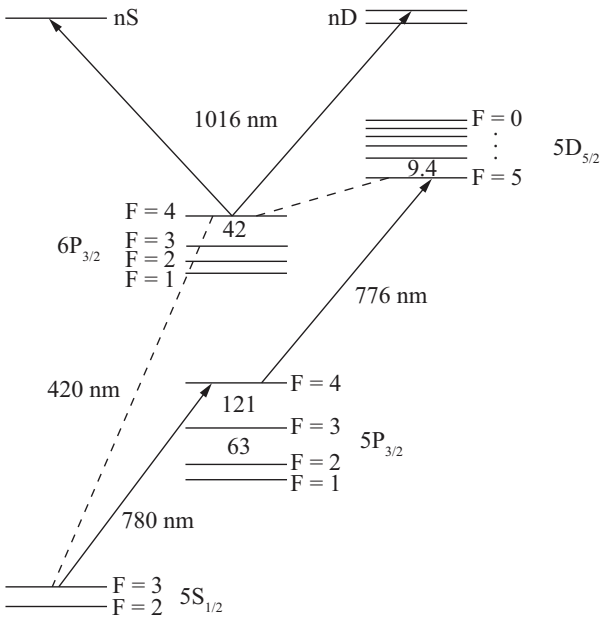

Fig. 1. Energy level scheme for the excitation of ^{85}Rb to Rydberg states. Included are the relevant hyperfine splittings (shown in MHz) and fluorescent transitions (dashed lines). By exciting only the $5P_{3/2}(F = 4) \rightarrow 5D_{5/2}(F' = 5)$ transition in the second step, only the $6P_{3/2}(F = 4)$ level is populated, thus allowing for a well-defined pathway to *n*S or *n*D states.

of the ^{85}Rb $nP_{3/2}$ [28] and by Johnson *et al.* to measure the absolute frequency of the ^{85}Rb $nF_{7/2}$ [29] Rydberg states.

We present an alternative diode laser system for three-step excitation to Rydberg states in ^{85}Rb (see Fig. 1). Both *n*S and *n*D states are accessible and with the application of a modest electric field, *n*P states can be excited. All three diode lasers operate at near-IR wavelengths (780 nm, 776 nm, and 1016 nm). The experiments presented here were perfomed in a rubidium MOT which traps and cools on the 5S→5P transition at $\lambda = 780$ nm. This transition also serves as the first step of our excitation scheme. The 5P→5D transition is driven by a Sharp GH0781JA2C 784 nm 120 mW laser diode cooled to operate at $\lambda = 776$ nm. Atoms may cascade to the ground state either through the $5P_{3/2}$ or $6P_{3/2}$ states. The final transition to Rydberg levels is from the $6P_{3/2}$ state with laser light near $\lambda = 1016$ nm.

The 5S→5P→5D two-photon transition has been extensively studied. Since the resonsant frequencies of the two transitions are nearly equal, the Doppler shifts for each nearly cancel when counterpropagating beams are used [30]. Two-photon excitation is possible for a large range of detunings from the intermediate 5P level, as seen in [31]. Additionally, the linewidth is mainly determined by the width of the final $5D_{5/2}$ state which is quite narrow (0.66 MHz). It has been shown that trapped atoms can be excited to the $5D_{5/2}$ state with more than 80% efficiency by the use of a counter-intuitive pulse sequence [32]. Furthermore, atoms in the $5D_{5/2}$ state can undergo superfluorescence through the $6P_{3/2}$ state [33]. Recently the lifetimes of the $5D_{3/2}$ and $5D_{5/2}$ states were measured to be 246.3(1.6) ns and 238.5(2.3) ns respectively [34], and the measured lifetime of the 6P manifold was found to be 120.7(1.2) ns [35].

A schematic of our laser setup is shown in Fig. 2. For the experiments presented in this work the trapping and cooling lasers are always on, and drive the first step ($5S_{1/2} \rightarrow 5P_{3/2}$) in

#147515 - $15.00 USD Received 13 May 2011; revised 27 Jun 2011; accepted 31 Jul 2011; published 16 Aug 2011

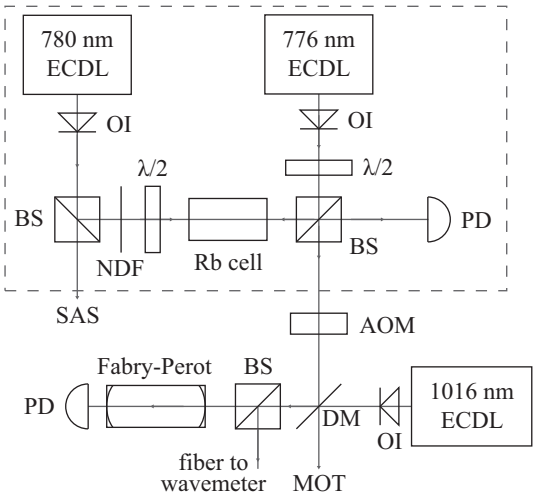

Fig. 2. Schematic of the laser system. A 780 nm ECDL is stabilized by saturated absorption spectroscopy (SAS, not shown) and used to lock a 776 nm ECDL to the $5P_{3/2} \rightarrow 5D_{5/2}$ transition via electromagnetically induced transparency in a Rb vapor cell (boxed region). Optical isolators (OI) prevent unwanted feedback. The 776 nm beam is focused through an AOM and combined with light from a 1016 nm ECDL with a dichroic mirror (DM) before being sent to the MOT. A portion of the 1016 nm light is monitored with a Fabry-Perot interferometer and wavemeter.

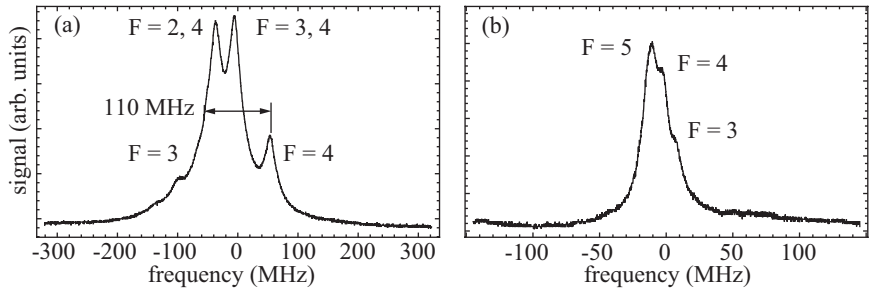

Fig. 3. (a) Saturated absorptions signal used to lock the 780 nm ECDL. (b) Nearly Doppler-free absorption spectrum of the $5P_{3/2} \rightarrow 5D_{5/2}$ used for locking the 776 nm ECDL.

the excitation scheme. The second transition is driven by an ECDL operating at $\lambda = 776$ nm, and a portion of this beam is used to stabilize its frequency. This is done by overlapping the 776 nm beam with a counterpropagating 780 nm beam in a rubidium cell. The Doppler-free electromagnetically-induced-transparency (EIT) [36] signal seen by monitoring the transmission of the 780 nm beam provides a useful locking signal for the 776 nm light. As discussed by Thoumany, *et al.* [27], the long lifetime of the $5D_{5/2}$ state results in quantum amplification of the absorption signal. The 780 nm beam is stabilized using conventional saturated absorption spectroscopy as shown in Fig. 3(a). The EIT signal used to lock the 776 nm laser is shown in Fig. 3(b).

In our arrangement, the $\lambda = 776$ nm beam is sent into the MOT from a single direction. The additional momentum provided by photons from this beam is sufficient to push atoms out of the MOT if it is not turned off periodically. To avoid this, we focus the $\lambda = 776$ nm beam through an acousto-optic modulator which allows for switching, but also shifts its frequency by 110 MHz.

#147515 - $15.00 USD Received 13 May 2011; revised 27 Jun 2011; accepted 31 Jul 2011; published 16 Aug 2011

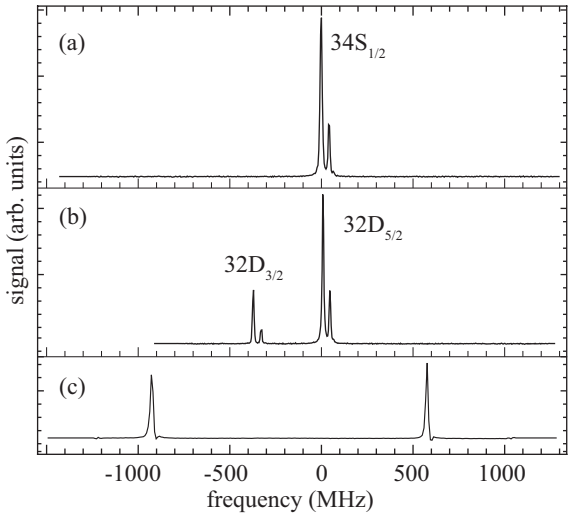

Fig. 4. Frequency scans of the (a) 32D doublet and (b) 34S state in the absence of an applied electric field. The larger peaks are due to excitation from the $6P_{3/2}(F=4)$ hyperfine level, while the smaller peaks are due to excitation from the $6P_{3/2}(F=3)$ hyperfine level. (c) A scan of the Fabry-Perot interferometer with a free-spectral range of 1.5 GHz.

To compensate for the 110 MHz frequency shift of the $\lambda = 776$ nm light before it enters the MOT, the $\lambda = 780$ nm diode laser is red detuned by the same amount and locked to the side of the $F = 2,4$ crossover peak. Thus our observed $5D_{5/2}$ spectrum includes hyperfine peaks for $F = 1-5$, whose individual separations ($<$10 MHz) are not fully resolved. Ideally, if the $\lambda = 776$ nm laser is tuned to the $F = 5$ hyperfine level, fluorescence to the $6P_{3/2}$ state should only populate the $F' = 4$ hyperfine level, thus ensuring a well-defined pathway. In practice, since the hyperfine levels of the $5D_{5/2}$ state are closely spaced, a limited fraction of atoms are excited to the $F = 4$ hyperfine level, which can fluoresce to either the $F' = 3$ or $F' = 4$ levels of the $6P_{3/2}$ state. This appears in our observed Rydberg spectra as a small feature spaced to higher energy by an amount equal to the $F' = 3,4$ energy separation ($\sim$42 MHz) [37]. Excitation to Rydberg states is done with an Axcel Photonics 1016 nm laser diode mounted in a home-built external cavity. Grating feedback allows for the operation of this laser over the range $\lambda = 1011-1030$ nm, as well as continuous single-mode tuning over a 2.5 GHz range. This allows access to Rydberg states between $n = 25$ and $n = 125$. A portion of the beam is measured with a Hewlett Packard 86120B Multi-Wavelength Meter to verify that it is tuned to the correct state, and the remainder (typically $\sim$70 mW) is combined with the $\lambda = 776$ nm beam before being sent into the MOT. After stabilization and modulation, the peak power of the $\lambda = 776$ nm beam entering the MOT is typically $\sim$5 mW.

Following excitation, Rydberg atoms are detected by field ionization. A high voltage pulse is applied to the trap $\sim 2\ \mu$s after the $\lambda = 776$ nm beam is turned off, and the resulting electrons are accelerated toward a chevron microchannel plate assembly where they are detected. For each shot we integrate the total detected atom signal. Repeated scans of the $\lambda = 1016$ nm laser frequency are made, and the resulting scans are averaged. In Fig. 4(a) we show the results of averaging 50 scans over the 34S state. The doublet that appears is due to excitation from two different hyperfine states of $6P_{3/2}$, $F = 3$ and 4, as mentioned earlier. In fact, close inspection of this signal reveals a very small additional peak consistent with excitation from the $6P_{3/2}$ $F = 2$ state. In Fig. 4(b) our laser is tuned to excite the 32D doublet. The spacing between

#147515 - $15.00 USD Received 13 May 2011; revised 27 Jun 2011; accepted 31 Jul 2011; published 16 Aug 2011

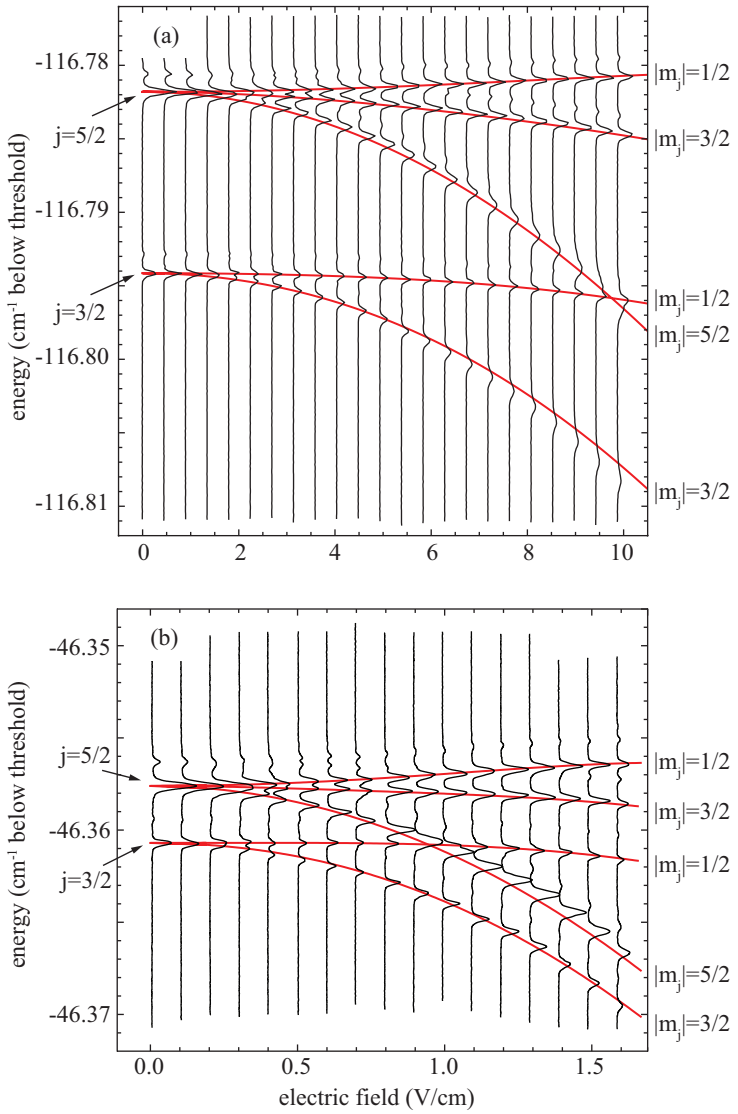

Fig. 5. Stark map for (a) the 32D and (b) the 50D states in ^{85}Rb. Shown in red is the calculated energy level splitting.

the two largest features is ∼380.3 MHz, in good agreement with the calculated $j = \frac{5}{2}, \frac{3}{2}$ fine structure splitting. Once again, we see pairs of states due to the excitation for the the two different hyperfine states of $6P_{3/2}$. To provide a calibration of our frequency scans, a portion of the $\lambda = 1016$ nm beam is sent into a ThorLabs confocal Fabry-Perot interferometer with a free-spectral range of 1.5 GHz as shown in Fig. 4(c). The narrowest measured linewidth is roughly 8 MHz (FWHM).

We also observed the Stark effect energy level splitting by performing frequency scans for a range of applied dc electric fields [38]. Experimentally obtained spectra overlayed with the calculated Stark maps for the 32D and 50D states are shown in Figs. 5(a) and (b), respectively. In both cases, the $|m_j|$ degeneracy breaking is clearly resolved and the observed spectra match

#147515 - $15.00 USD Received 13 May 2011; revised 27 Jun 2011; accepted 31 Jul 2011; published 16 Aug 2011

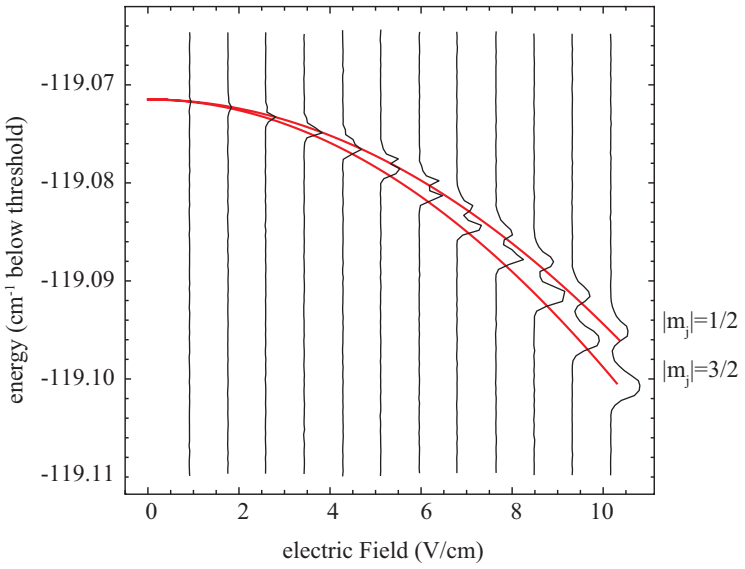

Fig. 6. Stark map for the $33P_{3/2}$ state in ^{85}Rb. Shown in red is the calculated energy level splitting.

the calculated splitting. Stark maps are calculated using the quantum defects measured by Li *et al.* [39].

Additionally, we used the mixing of states due to the Stark effect to observe atoms whose energy levels are adiabatically connected to the zero-field 33P state. Figure 6 shows the Stark splitting of the $33P_{3/2}$ state in a dc electric field. As the electric field is brought to zero, the number of detected 33P atoms diminish, until a signal is no longer observable below about 1 V/cm. The $33P_{1/2}$ state is not shown because the $j = \frac{3}{2}, \frac{1}{2}$ splitting for the 33P state is larger than the single-mode tuning range of our laser.

Finally, we investigated the degree to which excitation is affected by the use of pulsed light for the final step. The $\lambda = 1016$ nm beam was pulsed by tightly focusing it through an AOM, and its first-order output was collimated and combined with the $\lambda = 776$ nm beam before being sent to the MOT. With the $\lambda = 1016$ nm laser tuned and locked to the $32D_{5/2}$ state with a stable confocal Fabry-Perot cavity, its pulse length was scanned from 30 ns to 17.94 μs and the total integrated signal of all ionized atoms was recorded. The length of the $\lambda = 776$ nm pulse was extended to 30 μs so that at a minimum it turned on 12 μs before the $\lambda = 1016$ nm pulse, and the end of both pulses were made to coincide. The results in Fig. 7 show fraction of trapped atoms that are excited as a function of pulse width, revealing a rapid rise as the pulse width increases to ~ 1 μs followed by saturation at about 10% excitation and then a second increase to around 20% excitation. Both the 776 nm and 1016 nm laser beams were weakly focused so that their size was larger than that of the trapped ball of atoms. The fraction of excited atoms could then be accurately quantified by measuring the loss of atoms from the trap after excitation and field ionization. This was done by collecting the fluorescence from the trapped atoms with a large numerical aperture lens on an avalanche photodiode and measuring the fluorescence signal just before and just after excitation. Since field ionization completely removes the atoms from the trap we ran our excitation sequence at a rate of 0.33 Hz so that the trap had adequate time to refill after each excitation.

Using the matrix elements and lifetimes quoted in [40] we have calculated the expected

#147515 - $15.00 USD Received 13 May 2011; revised 27 Jun 2011; accepted 31 Jul 2011; published 16 Aug 2011

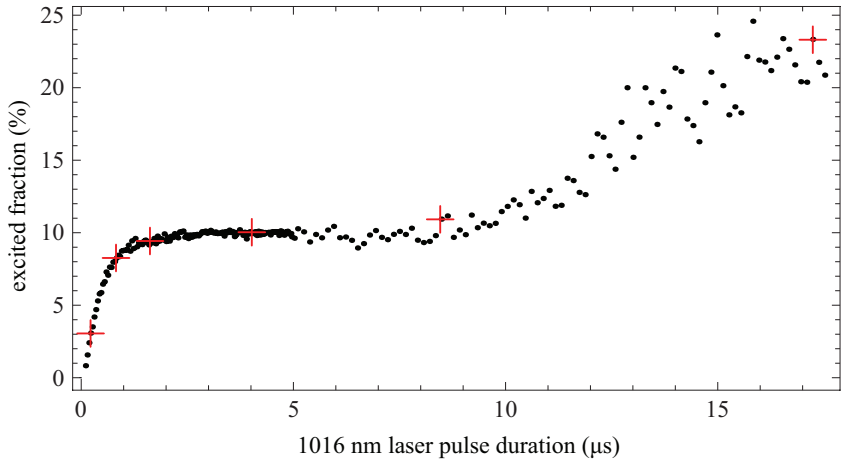

Fig. 7. Integrated signal for $32D_{5/2}$ Rydberg state excitation for 1016 nm pulse durations ranging from 50 ns to 5.14 μs in 20 ns increments.

saturation level for the *n*D Rydberg state to be 4%, well below the observed level. The reason for the excess excitation is revealed in the time resolved electron signal from our field ionized atoms shown in Fig. 8. We field ionize the Rydberg atoms with a slowly rising (~ 1 μs) electric field pulse. With this pulse, more tightly bound atoms will ionize at a larger field and thus later in time than weakly bound atoms. For a short 1016 nm excitation pulse we see a narrow feature (with some ringing) arriving at the detector at a time that we correlate with atoms that were in the 32D Rydberg state. For a 0.82 μs pulse the field ionization signal broadens and we see several peaks arriving earlier in time, indicating that additional states are being populated. These states are not populated directly by the 1016 nm laser, whose wavelength remains fixed, but rather through energy exchange due to the strong long-range interactions among atoms [41]. For longer excitation pulses the population continues to spread among a range of Rydberg states. At a pulse duration of 8.42 μs a new feature appears, a narrow spike that arrives at a time coincident with the beginning of our field ionization pulse. This is the signature of an ultracold plasma [14, 42]. In this case the strong dipole-dipole interaction between atoms has caused some to collide and ionize. The initially ionized electrons exit the trapping region leaving the positive ions behind. Eventually the potential well formed by these cold ions is large enough to trap the collisionally ionized electrons forming an ultracold plasma. A weak electric field is sufficient to extract the electrons from the plasma producing the prompt peak in our field ionization signal. At 17.24 μs the system has completely evolved into an ultracold plasma. Our simple rate equation model, which predicts a steady state excitation of 4%, does not account for any redistribution of Rydberg states. In effect this redistribution is an open channel that allows atoms to be removed from the excitation cycle thus increasing the total fraction of atom lost from the trap.

In conclusion, we have demonstrated a diode laser system capable of exciting ^{85}Rb to *n*S and *n*D Rydberg states, as well as *n*P states with the application of a modest electric field. It was shown that for the 32D, 50D, and $33P_{3/2}$ states both the fine structure splitting and Stark splitting in a dc electric field can be completely resolved. Excitation pulses as short as 30 ns were also feasible with this system due to the power available by the last step in the excitation process.

This system nicely complements other systems that have recently been developed by providing access to Rydberg states using near infrared lasers without the need for second harmonic

#147515 - $15.00 USD Received 13 May 2011; revised 27 Jun 2011; accepted 31 Jul 2011; published 16 Aug 2011

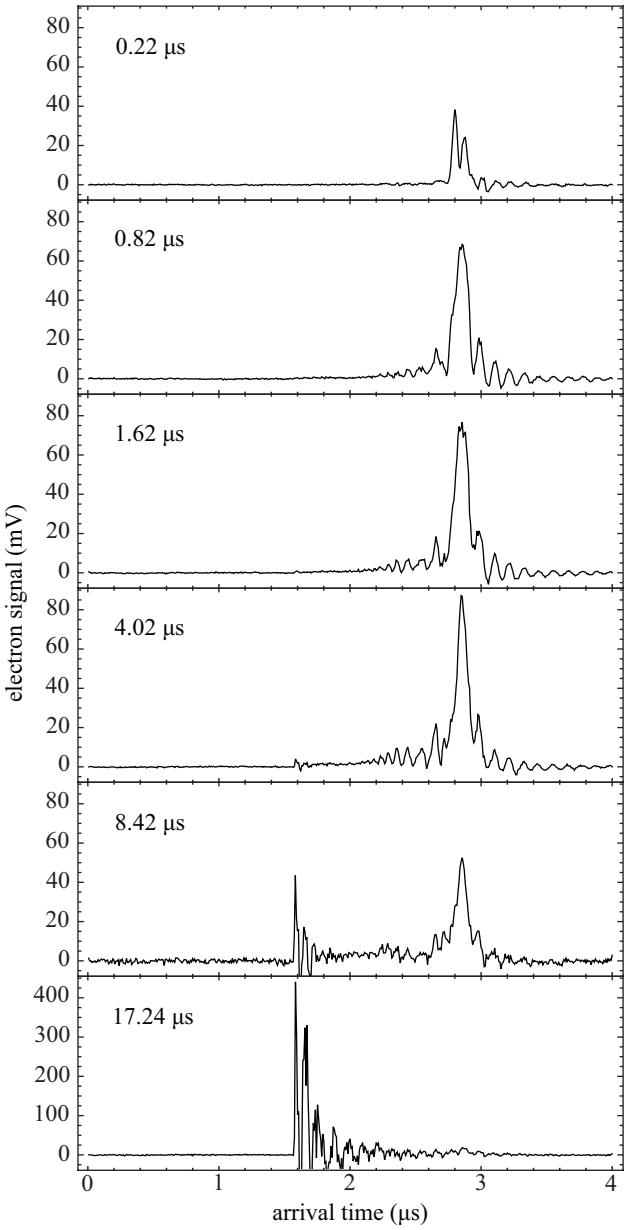

Fig. 8. Time resolved electron signals from the field ionized Rydberg atoms for several 1016 nm excitation pulse durations. Each panel is labeled with the duration of the excitation pulse used, which is also marked with a red cross in Fig. 7.

#147515 - $15.00 USD Received 13 May 2011; revised 27 Jun 2011; accepted 31 Jul 2011; published 16 Aug 2011

generation. This is acheived in our system through a three-step excitation scheme, whereas two-step pathways involving blue light often require frequency doubling an infrared laser diode, thereby significantly complicating the laser system. The other three-step system that has been used to excite Rydberg states of ^{85}Rb couples to nP and nF states in zero electric field, whereas our system couples to nS and nD states. States of other angular momenta could be excited by Stark mixing in a modest electric field. One limitation of our system is the necessary radiative step, which eliminates the possibility of coherent pulsed excitation schemes and limits the linewidth of the observed transitions. In spite of these limitations we expect this laser system will be a useful tool for the study of ultracold Rydberg atoms. We note that decoupling the trapping lasers from our excitation scheme would provide more control over the excitation of the intermediate 5D state.

Acknowledgments

This material is based upon work supported by the National Science Foundation under Grant No. 0653544. We also thank Thomas J. Carroll for providing the calculated Stark maps.

#147515 - $15.00 USD Received 13 May 2011; revised 27 Jun 2011; accepted 31 Jul 2011; published 16 Aug 2011